Research on Attitude Analysis of Hydraulic Support Based on Column Length

Mingfei Mu[1] – Bowen Xie[1] – Yang Yang[1,2,3,*]

[1] Shandong University of Science and Technology, College of Mechanical and Electrical Engineering, China
[2] Shandong Provincial Key Laboratory of Mining Mechanical Engineering, China
[3] Collaborative Innovation Center of Mine Intelligent Equipment and Technology, China

The existing hydraulic support attitude monitoring and control methods integrate multiple sensing technologies, but it is difficult to apply and promote due to unclear monitoring mechanisms, complicated types, and a large number of sensors. Aiming at the problem of attitude monitoring and control of hydraulic support, firstly, the kinematics mathematical model of hydraulic support is established by the key marker point method and the two-dimensional bar system model, and the forward and inverse solution algorithm of hydraulic support attitude based on the double-drive length of front and rear columns is proposed. Secondly, the rigid body dynamics simulation model of hydraulic support is constructed to verify the theoretical analytical model and prove the correctness of the algorithm. The rigid body simulation model can be used as the attitude monitoring system of hydraulic support. Thirdly, considering the influence of material elastic deformation, a rigid-flexible coupling dynamic simulation model of hydraulic support is established to explore the influence of elastic deformation of components on the attitude of hydraulic support and its causes. On this basis, the rigid-flexible coupling dynamic simulation model of the hydraulic support with clearance is established by replacing the revolute pair in the simulation model with the solid axis pin connection unit. The influence of the axis pin connection clearance on the attitude of the hydraulic support and its causes are explored, and the actual attitude and change characteristics of the hydraulic support under simulated real conditions are obtained. Finally, considering the force compression of the hydraulic cylinder of the column, the rigid-flexible and machine-liquid coupling dynamic simulation model of the hydraulic support with clearance is constructed. The loading test proves that the force compression of the hydraulic cylinder has a great influence on the attitude of the hydraulic support, indicating that when adjusting the attitude of the hydraulic support, the theoretical flow calculation cannot be used, and the column length should be directly measured. In this paper, the analytic method of the hydraulic support attitude is studied and verified using numerical calculation and simulation analysis, and the rigid-flexible coupling dynamic simulation model is built to study the various factors affecting the hydraulic support attitude. The research results of this paper can provide a theoretical basis and technical support for the attitude monitoring and control of hydraulic support.
Keywords: analysis of hydraulic support attitude, simulation analysis, rigid-flexible coupling, axis pin connection clearance, hydraulic cylinder stiffness

Highlights
- *The forward and inverse solution algorithm of hydraulic support attitude based on front and rear columns double drive length is proposed, and a method of hydraulic support attitude monitoring and control based on column length is proposed.*
- *The influence of material elastic deformation and axis pin connection clearance on the attitude of hydraulic support and its causes are explored, and the actual attitude and variation characteristics of hydraulic support under simulated real conditions are obtained.*
- *Considering the force compression of the column hydraulic cylinder, the rigid-flexible and machine-liquid coupling dynamic simulation model of the hydraulic support with clearance is constructed, and the influence of the force compression of the hydraulic cylinder on the attitude of the hydraulic support is explored through the loading test.*

0 INTRODUCTION

With the National Development and Reform Commission and eight other ministries and commissions jointly issuing "guidance on accelerating the intelligent development of coal mines", China's intelligent coal mine construction has entered a new stage [1] to [3]. The intelligent mining technology of the working face, which is mainly characterized by intelligent, cooperative control of a fully mechanized mining equipment group, is the key to the construction of intelligent coal mines [4]. Hydraulic support is an important supporting equipment of fully mechanized mining face in the process of coal production. It is one of the key electromechanical equipment to realize the "few people" and "unmanned" of a fully mechanized mining face, which directly affects the production safety and mining efficiency of the whole fully mechanized mining face. Hydraulic supports play a crucial role in achieving automatic and intelligent mining on fully mechanized faces by providing adaptive support to the surrounding rock [5] and [6]. The ability of these supports to intelligently detect and precisely evaluate their position and attitude is fundamental to their effectiveness in adapting to the

*Corr. Author's Address: College of Mechanical and Electrical Engineering, Shandong University of Science and Technology, Qingdao, China, yang.yang@sdust.edu.cn

293

surrounding rock. However, challenges in this area remain unresolved.

To promote the intelligent development of coal mining and ensure the normal support attitude of hydraulic support, many experts and scholars at home and abroad have carried out research on the monitoring and control technology of hydraulic support attitude. Ren et al. [7] used multi-sensor measurement technology to collect 15 independent parameters of the full-position attitude of a fully mechanized mining equipment group and designed a multi-parameter measurement system for a full-position attitude of a fully mechanized mining equipment group. Li and Ren [8] pointed out that the measurement effect of the existing measurement technology is greatly affected by the geological conditions of the working face, and the measurement accuracy, comprehensiveness, and automation of the measurement parameters need to be further improved. Most mines still need to adopt traditional manual measurement methods. Pang et al. [9] proposed an analytical method for the attitude and height of hydraulic support based on the column jack stroke and the balance jack stroke drive and used three calculation methods for attitude analysis. Wang et al. [10] used UNITY3D software to establish the multi-axis pin constraint model of hydraulic support and realized the attitude solution and monitoring of hydraulic support under different axis pin clearance. Chen et al. [11] applied the fusion technology of wide-angle ultrasonic sensors and inclination sensors to the attitude monitoring of hydraulic support. Zhang et al. [12] proposed a hydraulic support attitude detection method based on the principle that three points can determine a plane. Liang et al. [13] used a grating tilt sensor to realize online hydraulic support attitude monitoring and proposed an error compensation method for tilt monitoring. Zeng et al. [14] used automated dynamic analysis of mechanical systems) (ADAMS) software to construct a numerical simulation model of hydraulic support and study the position and dynamic response of hydraulic support under double impact load. Ge et al. [15] used the virtual software Unity 3D to construct the coal mining working environment and realized the adjustment of the supporting attitude of the hydraulic support to the surrounding rock of the coal seam in the virtual environment. Wang et al. [16] used three red-green-blue-depth (RGB-D) cameras to obtain the point cloud of the hydraulic support from different angles to obtain the complete point cloud information of the hydraulic support and realize the attitude and straightness measurement of the hydraulic support group. Yang et al. [17] designed a novel method for measuring the attitude and straightness of hydraulic support based on the "motion process recovery method" and established an automatic online measurement system. According to the complementary characteristics of a magnetometer, accelerometer, and gyroscope, Lu et al. [18] designed a supporting attitude sensing system composed of an inertial measurement unit and micro-electro-mechanical system (MEMS). Wang et al. [19] and [20] proposed a real-time virtual monitoring method for intelligent, fully mechanized mining faces by using virtual reality monitoring technology and carried out intelligent monitoring of fully mechanized mining face driven by (VR) augmented reality (AR) and virtual reality (VR) fusion. Szurgacz et al. [21] introduced a new method for monitoring and detecting the cross-section geometry of hydraulic support based on a new measurement system for the torsion angle of mechanical elements of hydraulic support cross-section. The posture of hydraulic support is calculated based on the tilt angle of the roof beam, base beam, shield beam, and four-bar mechanism obtained with the tilt sensor. Szurgacz et al. [22] proposed hydraulic support design and test methods based on predicted loads affecting roof supports, selected support types, support component testing, and allowable support operating conditions, and based on analysis of safety and control systems, develop an integrated method for testing and evaluating the possibility of using hydraulic supports under specific mining and geological conditions.

The above research provides theoretical and engineering practice support for the attitude detection of hydraulic support. However, most of the existing detection methods use sensors to directly detect the attitude of executive parts such as the roof beam and shield beam or use a variety of sensor signal fusion methods to obtain the attitude information of hydraulic support. This leads to the use of a variety of sensors, a large number of sensors, and a high cost, which is not conducive to wide application. Moreover, these studies did not consider the impact of stent deformation and other factors on stent attitude monitoring.

To monitor and control the attitude of hydraulic support better and further explain the cause of attitude error of hydraulic support, an analytical model of hydraulic support attitude theory based on the length of front and rear columns is proposed. The attitude information of the whole hydraulic support can be obtained by the length of the front and rear columns. The support height and the inclination angle of each component can be calculated by the length of the front and rear columns. The length of the front and

rear columns can also be calculated using the support height and the inclination angle of the top beam to guide the attitude monitoring and control of the hydraulic support. The theoretical analytical model is verified by the simulation to ensure its accuracy and reliability, and three factors that may affect the monitoring and control accuracy are analysed to determine the influence of different factors on the analytical accuracy. The research results provide a more efficient method for attitude monitoring and control of hydraulic support, theoretical support for attitude analysis error analysis of hydraulic support, and in-depth technical support for attitude research of hydraulic support.

The main scientific contributions of this paper are as follows:

1. An algorithm for calculating the attitude of hydraulic support based on the double driving length of the front and rear columns is proposed, and a method for monitoring and controlling the attitude of hydraulic support based on the length of columns is further proposed.

2. The influence of elastic deformation of material and pin joint clearance on the attitude of hydraulic support and its causes are discussed, and the actual attitude and change characteristics of hydraulic support under simulated real conditions are obtained.

3. The hydraulic cylinder's force compression is considered and the rigid-flexible mechanical-hydraulic coupling dynamic simulation model of hydraulic support with clearance is established.

The detailed work of this paper is as follows. Section 1 establishes the kinematics mathematical model of hydraulic support, puts forward the forward and inverse solution algorithm of hydraulic support attitude based on double drive length of front and rear columns, and puts forward a method of hydraulic support attitude monitoring and control based on column length. Section 2 establishes the rigid body dynamics simulation model of hydraulic support and verifies the theoretical analysis model. Section 3 establishes the rigid-flexible coupling dynamic simulation model of hydraulic support to explore the influence of elastic deformation of components on the attitude of hydraulic support and its causes. Section 4 establishes the equivalent prototype of hydraulic support and further verifies the theoretical analysis model of hydraulic support attitude and the rigid body dynamics simulation model of hydraulic support through experiments. Section 5 establishes the rigid-flexible coupling dynamics simulation model of hydraulic support with clearance to explore the

influence of pin clearance on the attitude of hydraulic support and its causes. Section 6 establishes the rigid-flexible and mechanical-hydraulic coupling dynamic simulation model of hydraulic support with clearance considering compression of the hydraulic cylinder and studies the influence of compression of the hydraulic cylinder on the attitude of hydraulic support through a loading test. Section 7 provides conclusions.

1 ANALYTICAL MODEL CONSTRUCTION OF HYDRAULIC SUPPORT ATTITUDE THEORY

1.1 Hydraulic Support Kinematics Mathematical Model Construction

The main moving parts of the four-column top coal caving hydraulic support include the base, the top beam, the shield beam, the front column, the rear column, the front connecting rod, and the rear connecting rod. The components are connected by axis pins, as shown in Fig. 1. The front column and the rear column are the driving components. The hydraulic cylinders of the two can be regarded as two sliding joints because they belong to two different kinematic branches; the hydraulic support can be regarded as a parallel robot with a top beam as an actuator [23].
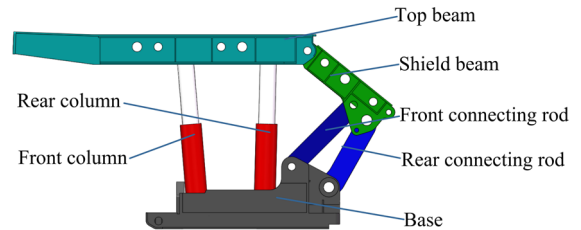

Fig. 1. *Four-column top coal caving hydraulic support main motion mechanism diagram*

The formula for calculating the degree of freedom of parallel mechanism is [24] and [25]

$$F = s \times (n - m - 1) + \sum_{i=1}^{m} f_i - v - q, \qquad (1)$$

where s *is* the order of the mechanism, $s = 6 - \lambda$, λ the number of public constraints of the institution, n the number of components of the mechanism, m the number of motion pairs of the mechanism, f_i the number of relative degrees of freedom of the ith motion pair, v the number of virtual constraint, and q local degree of freedom of the mechanism.

There are three common constraints in hydraulic support, so $\lambda = 3$, The order of the mechanism $s = 6 - \lambda = 6 - 3 = 3$. There are nine main moving parts

and 11 motion pairs in the hydraulic support, so $n = 9$, $m = 11$. There are no virtual constraints and local degrees of freedom, so $v = 0$, $q = 0$. The degree of freedom of the main motion mechanism of the four-column top coal caving hydraulic support can be calculated by Eq. (1) as follows:

$$F = 3 \times (9 - 11 - 1) + 11 = 2. \qquad (1)$$

Since the hydraulic cylinders of the front and rear columns provide two drives, the number of drives is equal to the number of degrees of freedom, and the mechanism has a certain movement [26] and [27]. When the length of the front and rear columns is known, the support height and the inclination angle of each component can be calculated by the forward kinematics solution. When the support height and the inclination angle of the top beam are known, the length of the front and rear columns can also be calculated by inverse kinematics.

The virtual prototype of the hydraulic support is measured, and the axis pin connection clearance is not considered. According to the structural size, the equivalent two-dimensional bar diagram of the hydraulic support shown in Fig. 2 is drawn [28].
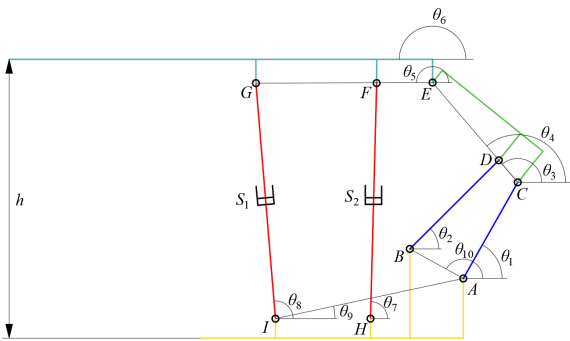

Fig. 2. *Hydraulic support equivalent two-dimensional bar diagram*

There are three kinematic chains from the base to the top beam, and the vector loop equations are

$$\begin{cases} \overline{AC} + \overline{CD} = \overline{AB} + \overline{BD} \\ \overline{HI} + \overline{IG} = \overline{HF} + \overline{FG} \\ \overline{IA} + \overline{AC} + \overline{CE} + \overline{EG} = \overline{IG} \end{cases} \qquad (2)$$

The nonlinear equations with S_1, S_2, and θ as variables can be obtained from this vector loop equation.

$$\begin{cases} L_{AC} \times \sin\theta_1 + L_{CD} \times \sin\theta_3 = L_{AB} \times \sin\theta_{10} + L_{BD} \times \sin\theta_2 \\ L_{HI} \times \sin\pi + S_1 \times \sin\theta_3 = S_2 \times \sin\theta_7 + L_{FG} \times \sin\theta_6 \\ L_{IA} \times \sin\theta_9 + L_{AC} \times \sin\theta_1 + L_{CE} \times \sin\theta_4 + L_{EG} \\ \quad \times \sin\theta_5 = L_{IG} \times \sin\theta_8 \\ L_{AC} \times \cos\theta_1 + L_{CD} \times \cos\theta_3 = L_{AB} \times \cos\theta_{10} + \\ L_{BD} \times \cos\theta_2 \\ L_{HI} \times \cos\pi + S_1 \times \cos\theta_3 = S_2 \times \cos\theta_7 + L_{FG} \times \cos\theta_6 \\ L_{IA} \times \cos\theta_9 + L_{AC} \times \cos\theta_1 + L_{CE} \times \cos\theta_4 + \\ L_{EG} \times \sin\theta_5 = L_{IG} \times \sin\theta_8 \\ \theta_{10} = \pi - \arctan\dfrac{265}{478} \\ \theta_3 = \theta_4 + 0.07 \\ \theta_5 = \theta_6 + 0.18 \end{cases} \qquad (3)$$

The distance from the front end of the top beam to the ground is the support height h, and the relationship between the support height h and other variables can be expressed as

$$\begin{cases} h = 175 + S_1 \times \sin\theta_8 + 213 \times \sin(\theta_6 - \dfrac{\pi}{2}) + 2207 \times \sin\theta_6 \\ h = 175 + S_2 \times \sin\theta_7 + 213 \times \sin(\theta_6 - \dfrac{\pi}{2}) + 3287 \times \sin\theta_6 \end{cases} . \quad (4)$$

The relationship between S_1, S_2 and h and other variables can be obtained by deformation.

$$\begin{cases} S_1 = \dfrac{h - 175 - 213 \times \sin(\theta_6 - \dfrac{\pi}{2}) - 2207 \times \sin\theta_6}{\sin\theta_8} \\ S_2 = \dfrac{h - 175 - 213 \times \sin(\theta_6 - \dfrac{\pi}{2}) - 3287 \times \sin\theta_6}{\sin\theta_7} \end{cases} . \quad (5)$$

For the forward solution, under the premise that S_1 and S_2 are known, the forward solution equations of kinematics can be obtained by combining Eqs. (3) and (4).

$$\begin{cases} L_{AC} \times \sin\theta_1 + L_{CD} \times \sin\theta_3 = L_{AB} \times \sin\theta_{10} + L_{BD} \times \sin\theta_2 \\ L_{HI} \times \sin\pi + S_1 \times \sin\theta_3 = S_2 \times \sin\theta_7 + L_{FG} \times \sin\theta_6 \\ L_{IA} \times \sin\theta_9 + L_{AC} \times \sin\theta_1 + L_{CE} \times \sin\theta_4 + L_{EG} \times \sin\theta_5 = L_{IG} \times \sin\theta_8 \\ L_{AC} \times \cos\theta_1 + L_{CD} \times \cos\theta_3 = L_{AB} \times \cos\theta_{10} + L_{BD} \times \cos\theta_2 \\ L_{HI} \times \cos\pi + S_1 \times \cos\theta_3 = S_2 \times \cos\theta_7 + L_{FG} \times \cos\theta_6 \\ L_{IA} \times \cos\theta_9 + L_{AC} \times \cos\theta_1 + L_{CE} \times \cos\theta_4 + L_{EG} \times \sin\theta_5 = L_{IG} \times \sin\theta_8 \\ \theta_{10} = \pi - \arctan\dfrac{265}{478} \\ \theta_3 = \theta_4 + 0.07 \\ \theta_5 = \theta_6 + 0.18 \\ h = 175 + S_1 \times \sin\theta_8 + 213 \times \sin(\theta_6 - \dfrac{\pi}{2}) + 2207 \times \sin\theta_6 \\ h = 175 + S_2 \times \sin\theta_7 + 213 \times \sin(\theta_6 - \dfrac{\pi}{2}) + 3287 \times \sin\theta_6 \end{cases} . \quad (6)$$

For the inverse solution, under the premise that the support height h and the top beam inclination angle θ_6 are known, the inverse solution equations can be obtained by combining Eqs. (3) and (5).

$$\begin{cases} L_{AC} \times \sin\theta_1 + L_{CD} \times \sin\theta_3 = L_{AB} \times \sin\theta_{10} + L_{BD} \times \sin\theta_2 \\ L_{HI} \times \sin\pi + S_1 \times \sin\theta_3 = S_2 \times \sin\theta_7 + L_{FG} \times \sin\theta_6 \\ L_{IA} \times \sin\theta_9 + L_{AC} \times \sin\theta_1 + L_{CE} \times \sin\theta_4 + \\ L_{EG} \times \sin\theta_5 = L_{IG} \times \sin\theta_8 \\ L_{AC} \times \cos\theta_1 + L_{CD} \times \cos\theta_3 = L_{AB} \times \cos\theta_{10} + L_{BD} \times \cos\theta_2 \\ L_{HI} \times \cos\pi + S_1 \times \cos\theta_3 = S_2 \times \cos\theta_7 + L_{FG} \times \cos\theta_6 \\ L_{IA} \times \cos\theta_9 + L_{AC} \times \cos\theta_1 + L_{CE} \times \cos\theta_4 + \\ L_{EG} \times \sin\theta_5 = L_{IG} \times \sin\theta_8 \\ \theta_{10} = \pi - \arctan\dfrac{265}{478} \\ \theta_3 = \theta_4 + 0.07 \\ \theta_5 = \theta_6 + 0.18 \\ h = 175 + S_1 \times \sin\theta_8 + 213 \times \sin(\theta_6 - \dfrac{\pi}{2}) + 2207 \times \sin\theta_6 \end{cases} \quad . (7)$$

$$\begin{cases} h = 175 + S_2 \times \sin\theta_7 + 213 \times \sin(\theta_6 - \dfrac{\pi}{2}) + 3287 \times \sin\theta_6 \\ S_1 \times \sin\theta_8 = h - 175 - 213 \times \sin(\theta_6 - \dfrac{\pi}{2}) - 2207 \times \sin\theta_6 \\ S_2 \times \sin\theta_7 = h - 175 - 213 \times \sin(\theta_6 - \dfrac{\pi}{2}) - 3287 \times \sin\theta_6 \end{cases} ,$$

1.2 Forward and Inverse Attitude Solution of Hydraulic Support Based on Iterative Approach Principle

In science and engineering, the solution of nonlinear equations is a very important topic. The traditional Newton iterative method and the string cut method have serious initial value dependence and local convergence. Therefore, in the process of forward and inverse solutions, the traditional analysis method is not used, but the *fsolve* function in MATLAB is used to numerically solve the two nonlinear equations. The *fsolve* function defaults to the trust-region-dogleg algorithm, and its core is to use the trust region to compensate for the limitations of the Newton method [29].

The nonlinear equations of forward solution are written into MATLAB, and the *fsolve* function is used for calculation. The forward solution algorithm is as follows [30] and [31].

$S_1 = 2119.2297; S_2 = 2112.7186;$
$f = @(x)([990 * \cos(x(1)) + 260.4611 * \cos(x(3)) -$
$546.5428 * \cos(pi - \arctan(265 / 478)) - 1125 * \cos(x(2));$

$990 * \sin(x(1)) + 260.4611 * \sin(x(3)) - 546.5428 *$
$\sin(pi - \arctan(265 / 478)) - 1125 * \sin(x(2));$
$850 * -1 + S_1 * \cos(x(8)) - S_2 * \cos(x(7)) -$
$1080 * \cos(x(6));$
$850 * 0 + S_1 * \sin(x(8)) - S_2 * \sin(x(7)) -$
$1080 * \sin(x(6));$
$1718.1385 * \cos(\arctan(360 / 1680)) + 990 * \cos(x(1)) +$
$1175.3931 * \cos(x(4)) + 1580 * \cos(x(5)) - S_1 * \cos(x(8));$
$1718.1385 * \sin(\arctan(360 / 1680)) + 990 * \sin(x(1)) +$
$1175.3931 * \sin(x(4)) + 1580 * \sin(x(5)) - S_1 * \sin(x(8));$
$0.00314 - x(5) + x(6);$
$0.00122 - x(3) + x(4);]);$
$x = fsolve(f, [1\ 1\ 1\ 1\ 3\ 3\ 1\ 1])$
$h = S_1 * \sin(x(8)) + 175 + 213 * \sin(x(6) - pi / 2) +$
$2207 * \sin(x(6))$
$qingjiao = x(6)$

After inputting the length S_1 and S_2 of the front and rear columns, the support height *h*, the top beam inclination angle *qingjiao,* and the inclination angle of each component are obtained.

Similarly, the nonlinear equations of the inverse solution are written into MATLAB, and the *fsolve* function is called to calculate. The inverse solution algorithm is as follows.

$h = 2500; p = pi;$
$f = @(x)([990 * \cos(x(1)) + 260.4611 * \cos(x(3)) -$
$546.5428 * \cos(pi - \arctan(265 / 478)) - 1125 * \cos(x(2));$
$990 * \sin(x(1)) + 260.4611 * \sin(x(3)) - 546.5428 *$
$\sin(pi - \arctan(265 / 478)) - 1125 * \sin(x(2));$
$850 * -1 + (h - 175 - 213 * \sin(p - pi / 2) - 2207 * \sin(p)) /$
$\sin(x(8)) * \cos(x(8)) - x(6) * \cos(x(7)) - 1080 * \cos(p);$
$850 * 0 + (h - 175 - 213 * \sin(p - pi / 2) - 2207 * \sin(p)) /$
$\sin(x(8)) * \sin(x(8)) - x(6) * \sin(x(7)) - 1080 * \sin(p);$
$1718.1385 * \cos(\arctan(360 / 1680)) + 990 * \cos(x(1)) +$
$1175.3931 * \cos(x(4)) + 1580 * \cos(x(5)) - (h - 175 - 213 *$
$\sin(p - pi / 2) - 2207 * \sin(p)) / \sin(x(8)) * \cos(x(8));$
$1718.1385 * \sin(\arctan(360 / 1680)) + 990 * \sin(x(1)) +$
$1175.3931 * \sin(x(4)) + 1580 * \sin(x(5)) - (h - 175 - 213 *$
$\sin(p - pi / 2) - 2207 * \sin(p)) / \sin(x(8)) * \sin(x(8));$
$0.00314 - x(5) + p;$
$0.00122 - x(3) + x(4);]);$
$x = fsolve(f, [1\ 1\ 1\ 1\ 3\ 2000\ 1\ 1])$
$S_1 = (h - 175 - 213 * \sin(p - pi / 2) - 2207 * \sin(p)) /$
$\sin(x(8))$
$S_2 = x(6)$

After inputting the support height h and the top beam inclination angle p, the lengths S_1 and S_2 of the front and rear columns are obtained.

1.3 Attitude Monitoring and Control Method of Hydraulic Support Based on Theoretical Analysis

In practical application, the displacement sensor can be used to monitor the length of the column to realize the attitude monitoring and control of the hydraulic support. For example, if you want to control the hydraulic support with a top beam angle to a certain support height, you only need to input the required support height and top beam angle into the forward solution program to obtain the required length of the front and rear columns, and then control the hydraulic system according to the reading of the displacement sensor. Drive the front and rear columns to the calculated length to complete the hydraulic support attitude control. Similarly, if you want to monitor the attitude of the hydraulic support, you only need to read the length of the front and rear columns through the displacement sensor and enter the forward solution program to obtain the height and angle information of the current top beam and the inclination angle of each component. The process continues to achieve continuous monitoring of the hydraulic support, and its monitoring and control process is shown in Fig. 3.
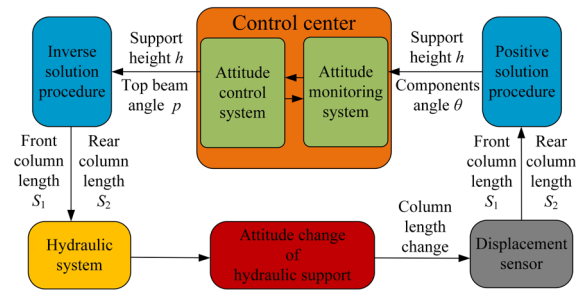

Fig. 3. *Hydraulic support attitude monitoring and control process*

2 VERIFICATION OF THEORETICAL ANALYTICAL MODEL OF HYDRAULIC SUPPORT BASED ON DYNAMIC SIMULATION

2.1 The Rigid Body Simulation Model of Hydraulic Support is Established

The three-dimensional model of the hydraulic support is imported into ADAMS through the ".xt" file interface. Rotating pairs are added at each hinge point of the hydraulic support, the direction is consistent with the direction of the hinge point rotation axis. Moving pairs are added between the piston rod and

hydraulic cylinder of the column and the tail beam jack, and the direction is consistent with the axial direction of the piston rod. Ball pairs are added between the column sockets of the column and the top beam and the base, and fixing pairs are added between the base and the ground, as shown in Fig. 4. Because this paper mainly studies the relationship between the front and rear columns and the attitude of the hydraulic support, a 0-size drive is added to the moving pair between the insert plate and the tail beam and between the insert plate and the tail beam to make it temporarily fixed, while the corresponding driving function is added to the moving pair on the four columns for simulation test.
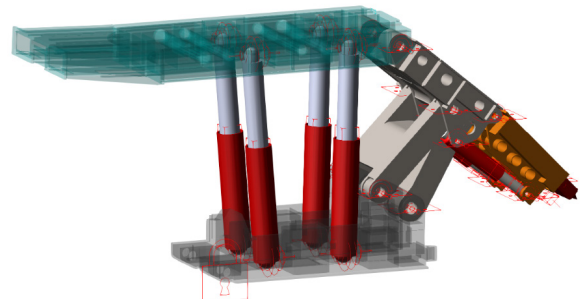

Fig. 4. *Rigid body simulation model of hydraulic support*

From 1700 mm to 2500 mm, a support height is taken every 10 mm, and the top beam inclination angle $p = pi$ is taken. The theoretical and analytical data of front and rear column lengths S_1 and S_2 under different support heights are input into MATLAB, respectively.

In ADAMS, a point drive is added to the top beam to make the top beam move downward horizontally. A reference quantity is taken every 10 mm from 0 mm to 800 mm to test, corresponding to the support height of 1700 mm to 2500 mm. The distance between the ball pairs at both ends of the front and rear columns is measured to obtain the simulation data of the length of the front and rear columns.

2.2 Verification of Theoretical Analytical Model of Hydraulic Support Based on Rigid Simulation

Some test data records the length of the front and rear columns at different support heights. Based on the simulation data, the inverse solution error of the theoretical analytical model is calculated, as shown in Fig. 5.
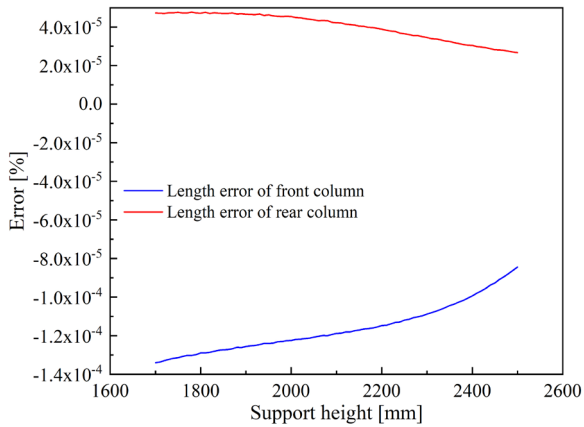
Fig. 5. *Error analysis of theory analytical inverse solution*

From the analysis of the results, the errors of the two are increasing with the decrease in support height. The maximum error of the length calculation of the front column appears when the support height is 1700 mm, which is -1.3397×10^{-4} %. The maximum error of the length calculation of the rear column appears when the support height is 1700 mm, which is 4.73114×10^{5} %. The error is very small, which can meet the requirements of regulating the attitude of hydraulic support through inverse kinematics. It is proved that the theoretical analysis method of inverse kinematics is correct, and the rigid body simulation model is correct.

Table 1. *Theoretical analysis and rigid body simulation support height data under different front and rear column lengths*

Length of front column [mm]	Length of rear column [mm]	Theoretical analysis data	Rigid body simulation data
		Support height [mm]	Support height [mm]
2100	2100	2467.1747	2467.1680
2000	2000	2365.7415	2365.7341
1900	1900	2265.1403	2265.1325
1800	1800	2164.7995	2164.7916
1700	1700	2064.3262	2064.3184
1600	1600	1963.4376	1963.4301
1500	1500	1861.9223	1861.9150
1400	1400	1759.6215	1759.6145

In MATLAB, the lengths S_1 and S_2 of multiple front and rear pillars are input into the forward solution algorithm to obtain the corresponding support height. In ADAMS, the drive is added to the moving pairs on the front and rear columns, respectively, so that the front and rear reach the corresponding length input in the forward solution algorithm, and the simulation data of the support height are measured, some data

of support height under different column lengths are shown in Table 1.

Based on the rigid body simulation data, the forward solution error of the theoretical analytical data is calculated, as shown in Fig. 6.
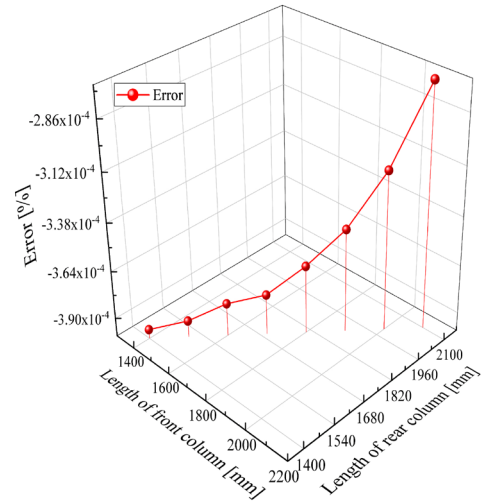

Fig. 6. *Error analysis of theory analytical forward solution*

From the analysis of the results, as the length of the front and rear columns decreases, the error of the support height increases; the maximum error is -3.9498×10^{-4} % when the length of the front and rear columns is 1400 mm. The error is very small, which can meet the requirements of regulating the attitude of hydraulic support through forward kinematics. It is proved that the theoretical analysis method of forward kinematics is correct, and the rigid body simulation model is correct.

The rigid body simulation model can be used as a hydraulic support attitude monitoring system. The real-time change of the hydraulic support attitude can be displayed by inputting the length data of the front and rear columns into the simulation system.

3 ATTITUDE ANALYSIS OF HYDRAULIC SUPPORT CONSIDERING DEFORMATION

3.1 Dynamic Simulation Model Construction of Rigid-Flexible Coupling Hydraulic Support

In the actual production process, although the length of the front and rear columns can be accurately monitored and used as a known quantity to calculate the hydraulic support's attitude information, the hydraulic support will inevitably deform due to its own weight and the pressure from the roof, which

will negatively impact the hydraulic support's attitude control and monitoring.

To make the simulation closer to the real working condition and explore the influence of component deformation on attitude control and monitoring of hydraulic support, a rigid-flexible coupling dynamic simulation model of hydraulic support is established, as shown in Fig. 7. In hyper-mesh software, mesh division is carried out on the top beam, shield beam, front connecting rod, rear connecting rod, tail beam and plugboard of hydraulic support through its pre-processing function [32] to [35]. Specific parameters of flexible body parts are as follows: mesh type: tetrahedral mesh, mesh size: 30 mm, material type: isotropic, elastic modulus E: 21000 MPa, shear modulus G: 81000 MPa, Poisson ratio: 0.3, density: 7860 kg/m³, constraint mode number: 6. After mesh division is completed, a flexible volume file with suffix '.mnf' is generated. Based on the rigid simulation model of hydraulic support established in Section 2.1, rigid parts are accurately replaced by corresponding flexible body parts by the "three-point method" [36] to [38], and flexible body parts are linked by rigid nodes and rotating pairs. In the rigid-flexible coupling dynamics simulation model of hydraulic support, the base and column are rigid parts, and the column is connected with the top beam and the column socket of the base by ball pairs. The piston rods and hydraulic cylinders of the front and rear columns are connected by a moving pair, and drive is added to the moving pair to drive the columns to present different lengths.
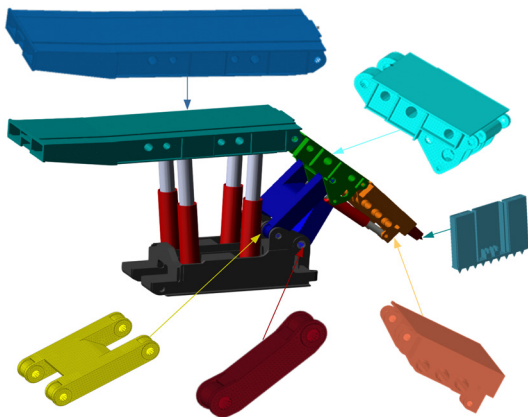

Fig. 7. *Rigid-flexible coupling dynamic simulation model of hydraulic support*

3.2 Attitude Error Analysis of Hydraulic Support Considering Material Deformation

The length of the front and rear pillars and the support height in the rigid body simulation data are taken, and the driving function of the front and rear pillars in the rigid-flexible coupling model of the hydraulic support is adjusted to make the front and rear pillars reach the multiple sets of test lengths in rigid body simulation in turn. The support height h is measured and recorded.

The attitude error of the rigid-flexible coupling simulation data is calculated based on the rigid body simulation data, as shown in Fig. 8.
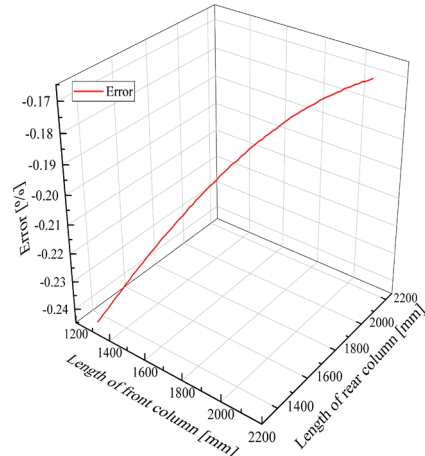

Fig. 8. *Rigid-flexible coupling dynamics simulation error of hydraulic support*

From the analysis of the results, the maximum error occurs when the length of the front column is 1323.0649 mm, the length of the rear column is 1323.0649 mm, and the error is -0.2412 mm. The minimum error is -0.1679 mm when the length of the front column is 2119.2297 mm, and the length of the rear column is 2112.7186 mm. The average error is -0.1948 mm. This error is only considering the weight of the hydraulic support, and the deformation of each component is small. If the hydraulic support is in the bearing state to bear the roof pressure, this error will be amplified. The error curve in Fig. 8. shows that as the length of the front and rear columns decreases, the error of the support height increases. To explore the causes of this trend, the force of the hinge points of each component at different heights is measured, and the force change curve is obtained, as shown in Fig. 9. From the curve, it can be seen that with the shortening of the front and rear columns, the height of the support decreases, and the force at the hinge point of the rear connecting rod-base, the rear connecting rod-shield beam and shield beam-top beam increases obviously. Due to the increase in force, deformation will inevitably increase, which will lead to an increase in error. This error is only considering the self-weight of the hydraulic support, and the deformation of each

component is small. If the hydraulic support is in the bearing state to bear the roof pressure, this error will be amplified. Therefore, in the process of monitoring or regulating the attitude of the hydraulic support, it is necessary to consider the error caused by the deformation of the hydraulic support.
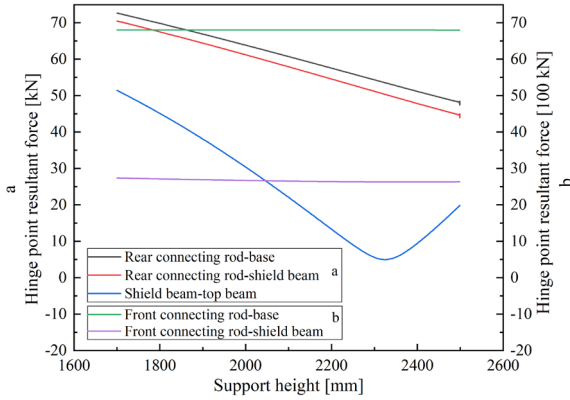

Fig. 9. *Hydraulic support rigid-flexible coupling dynamics simulation hinge point force analysis*

4 EXPERIMENTAL VERIFICATION OF ATTITUDE ANALYSIS BASED ON EQUAL SCALE PROTOTYPE OF HYDRAULIC SUPPORT

4.1 Establishment of Experimental System for Attitude Analysis of Hydraulic Support

According to the hinge position and component length of the two-dimensional rod system model of hydraulic support in Fig. 1, the equivalent prototype of each component of hydraulic support with equal scale of 20:1 is obtained, as shown in Fig. 10. Four column lengths of 2100 mm, 1900 mm, 1700 mm, and 1500 mm (the size in the equivalent prototype is 105, 95, 85, 75, respectively) are selected to obtain equivalent column links of four lengths as shown in Fig. 11.
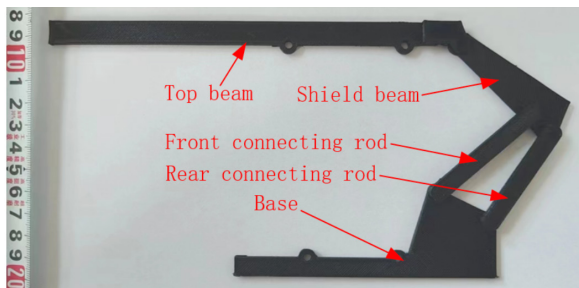

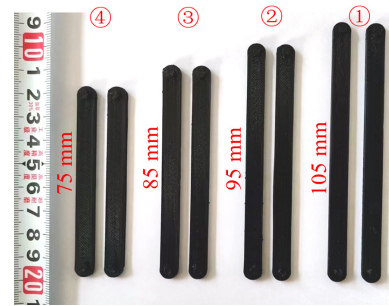**Fig. 10.** *Attitude analysis experimental system of hydraulic support*

Fig. 11. *Hydraulic support column equivalent links*

4.2 Inverse Solution Experiment of Hydraulic Support Attitude

Respectively adjust the support height of hydraulic support to 2500 mm, 2300 mm, 2100 mm, and 1900 mm (The size in the equivalent prototype is 125, 115, 105, and 95, respectively), and the top beam is parallel to the base plate. A vernier caliper is used to measure the column lengths S_1 and S_2 under four different heights, as shown in Fig. 12.
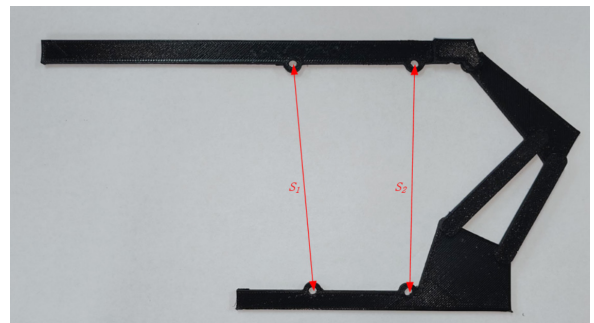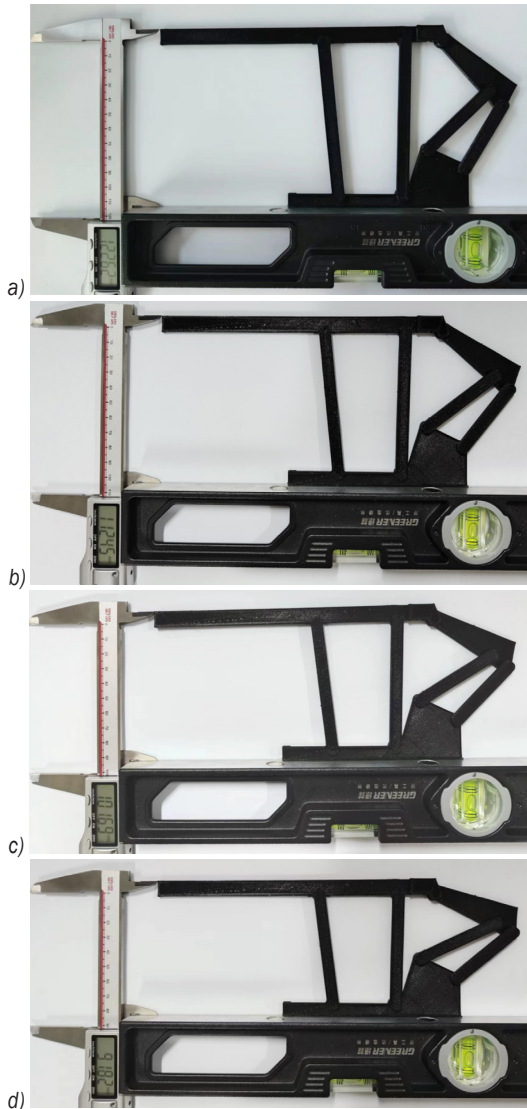

Fig. 12. *Inverse solution experiment of hydraulic support attitude*

4.3 Forward Solution Experiment of Hydraulic Support Attitude

The equivalent connecting rod for four kinds of column length is installed in the attitude analysis experimental system of hydraulic support, and the vertical distance (support height) from the front end of the top beam to the bottom of the base is measured by a vernier caliper. Thus, the support height parameters of hydraulic support under four kinds of column lengths are obtained, as shown in Fig. 13.

Fig. 13. *Forward solution experiment of hydraulic support attitude at column length: a) 105 mm, b) 95 mm, c) 85 mm, and d) 75 mm*

4.4 Analysis of Experimental Results of Attitude Analysis of Hydraulic Support

The length of the front and rear columns obtained from the inverse solution experiment of hydraulic support attitude is compared with the theoretical analysis value, and the error between them is analysed. The experimental analysis data are shown in Table 2.

According to the experimental results of the hydraulic support inverse solution, the theoretical analytical value is compared with the experimental value, and the error is less than 1 %.

The length of the front and rear columns obtained from the forward solution experiment of hydraulic

support attitude is compared with the theoretical analysis value, and the error between them is analysed. The experimental analysis data are shown in Table 3.

Table 2. *Comparison of inverse solution results*

Support height [mm]	Theoretical analysis [mm]		Experimental calculation [mm]		Error [%]	
	S1	S2	S1	S2	S1	S2
125	105.96	105.64	105.50	105.33	0.43	0.29
115	96.00	95.64	95.10	95.32	0.94	0.33
105	86.02	85.65	85.85	85.01	0.20	0.75
95	76.07	75.66	75.98	75.21	0.12	0.59

Table 3. *Comparison of forward solution results*

Column length [mm]	Theoretical analysis [mm]	Experimental calculation [mm]	Error [%]
105	123.36	122.62	0.60
95	113.26	112.45	0.72
85	103.22	101.69	1.48
75	93.10	91.82	1.37

According to the experimental results of the hydraulic support forward solution, the theoretical analytical value is compared with the experimental value, and the error is less than 1.5 %.

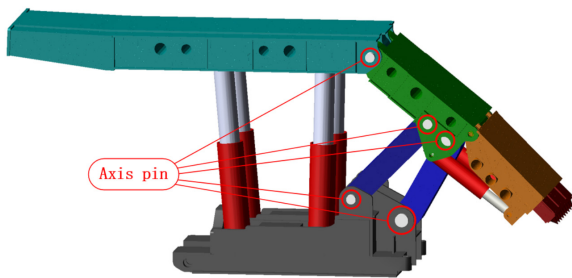### 5 ANALYSIS OF THE INFLUENCE OF CLEARANCE ON THE ATTITUDE OF HYDRAULIC SUPPORT

5.1 Construction of Rigid-Flexible Coupling Dynamics Simulation Model of Hydraulic Support with Clearance

Ideally, due to the four-link structure of the support, stable movement is achieved on the premise of maintaining stability. However, due to the constraints of production design, assembly error, friction, and wear, it is inevitable that there will be a clearance between the axis pin and the pinhole of each hinge point, which will affect the overall attitude of the support. In order to ensure the accuracy of attitude monitoring and control of hydraulic support [39] to [41], it is necessary to study it.

Based on the rigid-flexible coupling model of the hydraulic support in Fig. 7, in the third section, the revolute joints of the hinge points of each component are deleted, and then the axis pin is added at the shaft hole. The axis pin material, length, and size are shown in Table 4. Collision contact constraints are added between the axis pin and the two connected components, respectively. The rigid-flexible coupling dynamic simulation model of the hydraulic support with clearance is shown in Fig. 14.

Table 4. *Axis pin parameter*

| Position	Axis pinhole diameter [mm]	Axis pin diameter [mm]	Axis pin length [mm]	Axis pin material
Top beam Shield beam	101	100	500	40Cr
Shield beam Front connecting rod	101	100	380	40Cr
Shield beam Rear connecting rod	140	139	550	40Cr
Base Front connecting rod	101	100	380	40Cr
Base Rear connecting rod	140	139	550	40Cr

Fig. 14. *Rigid-flexible coupling dynamics simulation model of hydraulic support with clearance*

The lengths of the front and rear pillars are changed to the corresponding lengths of the support height of 2490 mm, which are 2109.2965 mm and 2102.7118 mm, respectively.

5.2 Analysis of Hydraulic Support Attitude Error Considering Axis Pin Connection Clearance

The change of support height with the length of the front and rear columns are shown in Fig. 15. From Fig. 15 it can be seen that the error between it and the rigid body simulation support height is about 2 mm. When the length of the front column is 2109.2965 mm, and the length of the rear column is 2102.7118 mm, the rigid-flexible coupling dynamics simulation support height of the hydraulic support with clearance is 2492.2649 mm, while the rigid body simulation support height is 2490 mm, and the error is 2.2649 mm. When the length of the front and rear columns just begins to decrease, the blue curve is below the red curve and then rises rapidly to the top of the red curve. The two curves intersect briefly. This is because the hydraulic support model is flexible except for the base. At the beginning of the simulation, the components are drooped by gravity, resulting in a decrease in the support height. Subsequently, because

the influence of the axis pin connection clearance on the attitude of the hydraulic support is much greater than the influence of the elastic deformation due to gravity, the support height increases rapidly. The tail end of the top beam is reduced due to the height of the axis pin clearance, and the length of the column is temporarily unchanged, resulting in the "head-up" phenomenon of the hydraulic support. This simulation model proves that the axis pin connection clearance has a great influence on the attitude monitoring and control of the hydraulic support, which is a factor that must be considered.
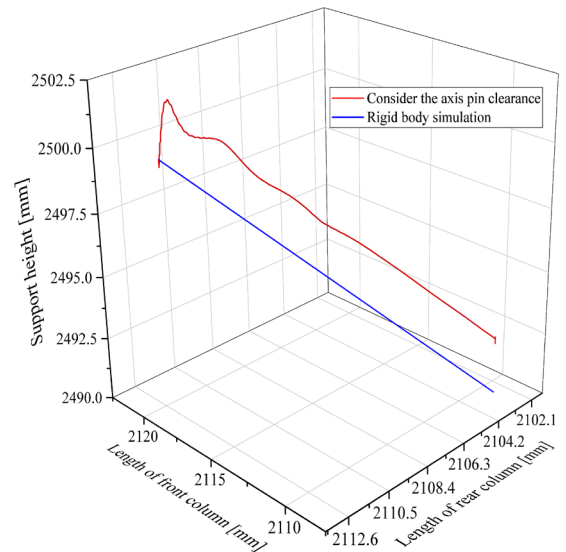
Fig. 15. *Comparison of support height between rigid-flexible coupling dynamics simulation and rigid body simulation of hydraulic support with clearance*

6 STUDY ON DYNAMIC PERFORMANCE OF RIGID-FLEXIBLE AND MACHINE-LIQUID COUPLING OF HYDRAULIC SUPPORT WITH CLEARANCE

6.1 Construction of Rigid-Flexible and Machine-Liquid Coupling Dynamics Simulation Model of Hydraulic Support with Clearance

When the attitude adjustment of the hydraulic support is carried out by calculating the theoretical flow, the force compression of the column hydraulic cylinder will lead to the deviation between the actual attitude and the expected attitude of the hydraulic support. Therefore, it is necessary to study the force compression and variable stiffness of the hydraulic cylinder before and after the hydraulic support.

In the hydraulic cylinder system of the front and rear columns, the volume of the hydraulic oil in the

hydraulic cylinder is not immutable when subjected to external pressure, and it is gradually compressed with the increase of external pressure, similar to the compressed spring, so the hydraulic oil in the rod cavity and the rodless cavity of the hydraulic cylinder can be equivalent to a certain stiffness spring. The stiffness of the hydraulic cylinder can be composed of two parts, one is the emulsion stiffness, and the other is the piston rod stiffness. Because the bulk modulus of the hydraulic oil is $Kv = 1.4$ GPa to 2 GPa, and the bulk modulus of the steel is between 196 GPa to 206 GPa, which is 100 to 150 times that of the hydraulic oil, the piston rod can be treated as a rigid body [42] to [44]. The structural characteristics of the hydraulic cylinder are shown in Fig. 16.
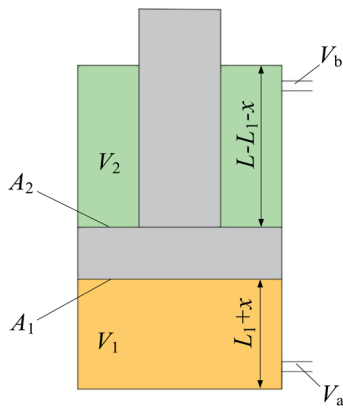

Fig. 16. *Column hydraulic cylinder structure diagram*

In Fig. 16 each symbol means: A_1 is the cross-sectional area of the rodless chamber piston of the hydraulic cylinder,
A_2 the cross-sectional area of the hydraulic cylinder rod cavity, L effective stroke of hydraulic cylinder, L_1 the current oil height of hydraulic cylinder rodless cavity, x vibrational displacement of the system, V_1 the volume of oil in rodless cavity of hydraulic cylinder, V_2 the volume of oil in the rod cavity of hydraulic cylinder, V_a the volume of oil in hydraulic cylinder rodless cavity hydraulic pipeline, and V_b the volume of oil in hydraulic cylinder rod cavity hydraulic pipeline.

The total equivalent stiffness of the hydraulic cylinder is

$$k = k_1 + k_2, \qquad (8)$$

where k_1 is the equivalent stiffness of oil in the rodless cavity and k_2 is the equivalent stiffness of oil in the rod cavity.

$$k = \frac{pA}{x}. \qquad (9)$$

The bulk modulus β_e of hydraulic oil is an important reference index for the classification and selection of hydraulic oil, which indicates the degree of compressibility of hydraulic oil in the hydraulic cylinder cavity. The larger the β_e, the more difficult the hydraulic oil in the hydraulic cylinder is to be compressed; the smaller the β_e, the easier the hydraulic oil in the hydraulic cylinder to be compressed. According to the compressible characteristics of hydraulic oil, the bulk modulus of hydraulic oil can be obtained as

$$\beta_e = \frac{pV}{dV} = \frac{pV}{Ax}. \qquad (10)$$

Substituting Eq. (10) into Eq. (9) can get:

$$k = \frac{\beta_e A^2}{V}. \qquad (11)$$

According to the structural characteristics of hydraulic cylinder

$$V_1 = (L_1 + x)A_1 + V_a, \qquad (12)$$

$$V_2 = (L - L_1 - x) \times A_2 + V_b. \qquad (13)$$

Substituting Eqs. (12) and (13) into Eq. (11) can get

$$k_1 = \frac{\beta_e A_1^{\,2}}{(L_1 + x)A_1 + V_a}, \qquad (14)$$

$$k_2 = \frac{\beta_e A_2^{\,2}}{(L - L_1 1x)A_2 + V_b}. \qquad (15)$$

Substituting Eqs. (14) and (15) into Eq. (8) can get

$$k = k_1 + k_2 = \frac{\beta_e A_1^{\,2}}{(L_1 + x)A_1 + V_a} + \frac{\beta_e A_2^{\,2}}{(L - L_1 - x)A_2 + V_b}. \qquad (16)$$

Since the values of x, V_a, and V_b are so small that they can be neglected in the calculation, Eq. (16) can be simplified to

$$k = \frac{\beta_e A_1}{L_1} + \frac{\beta_e A_2}{L - L_1}. \qquad (17)$$

The structural parameters of the column hydraulic cylinder are shown in Table 5.

Table 5. *Column hydraulic cylinder structure parameters*

Hydraulic cylinder type	Hydraulic cylinder inner diameter	Piston rod diameter	Hydraulic cylinder effective stroke
Single stretching	230	210	1071

Eq. (17) is input into MATLAB, and the effective stroke L_1 is 1071 mm. According to the piston rod diameter of 210 mm and the hydraulic cylinder diameter of 230 mm, $A_1 = 41547.5621$ mm², $A_2 = 6911.5037$ mm² is calculated. Taking 5 % emulsion as an example, $\beta_e = 1.82 \times 10^3$ MPa. Through MATLAB calculation, the oil height of the rodless cavity and the total equivalent stiffness curve of the column hydraulic cylinder are obtained, as shown in Fig. 17. It can be seen from the diagram that with the increase of the height of the rodless cavity oil, the total equivalent stiffness of the column hydraulic cylinder shows a trend of decreasing first and then increasing, and the slope is small and stable in the middle of 300 mm to 900 mm interval, while the slope is large and the change is fast in the 100 mm to 300 mm and 900 mm to 1000 mm intervals at both ends.
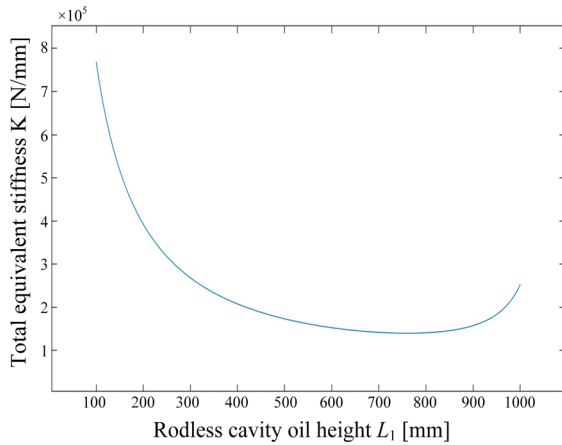

Fig. 17. *The change of total equivalent stiffness of column hydraulic cylinder*

The formula of oil height and column length can be obtained from the structure of the column hydraulic cylinder.

$$L_1 = L_0 - 1193, \qquad (18)$$

where L_0 is the total length of the column.

After measurement, the length of the front column is 2119.2297 mm, and the length of the rear column is 2112.7186 mm. The front column L_1 is 923.2297 mm, and the rear column L_2 is 919.7186 mm. Substituting L_1 and L_2 into Eq. (17), the equivalent stiffness of the front and rear columns is 168528.1897 N/mm and 165366.3258 N/mm.

Based on the rigid-flexible coupling dynamic simulation model of the hydraulic support with clearance in Fig. 14, the four columns of the front and rear groups are replaced by the spring damping system.

The stiffness of the spring damping system that replaces the front and rear columns is set to the calculated value of the current height, and the rigid-flexible and machine-liquid coupling dynamics simulation model of the hydraulic support with clearance is completed, as shown in Fig. 18.
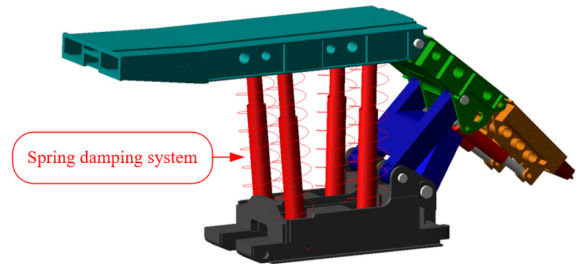

Fig. 18. *Rigid-flexible and machine-liquid coupling dynamics simulation model of hydraulic support with clearance*

The hydraulic support is statically loaded to test the attitude change of the support system under static load. Therefore, the static loading model of the hydraulic support is established as shown in Fig. 19.
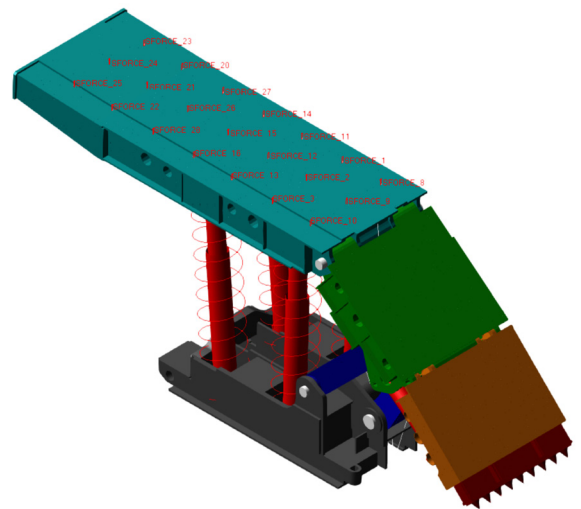

Fig. 19. *Static loading model of hydraulic support*

The rated working resistance of the hydraulic support studied in this paper is 5200 kN, so the vertical static load should be set to 5200 kN. Because the top beam is a flexible body, loading the working resistance directly at one point will cause abnormal deformation. Therefore, it is loaded with 21 loading positions at equal intervals. The force at each loading position is the same as 247619.0476 N, and the sum is the rated working resistance. The loading method is shown in Fig. 19. In order to avoid the formation of sudden load, the spring damping system makes

it difficult to restore the equilibrium state. The step function *STEP* (time, 0, 0, 0.5, 247619.0476) is used to increase the resultant force from 0 to the rated working resistance within 0.5 s, and the simulation time is set to 1 s.

6.2 Attitude Error Analysis of Hydraulic Support Considering Elastic Deformation of Hydraulic Cylinder

The change of the support height of the hydraulic support in the loading test is shown in Fig. 20. The support height begins to decrease from 2500 mm under the action of self-weight and working resistance, and finally stabilizes at 2409.1314 mm, and the reduction of the support height is 90.8686 mm. If it is loaded at other support heights, due to the change in hydraulic cylinder stiffness, the support height will change differently. The results show that in the process of attitude monitoring and regulation of hydraulic support if the length of the column is indirectly calculated by monitoring the flow, the actual attitude of the hydraulic support will have a great error with the expected attitude, which will have a negative impact on the attitude adjustment of the hydraulic support. Therefore, the theoretical flow calculation cannot be used when adjusting the attitude of the hydraulic support, and the length of the column should be directly measured.
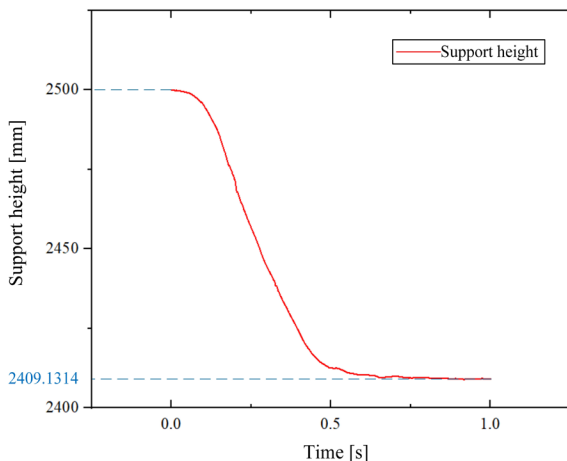

Fig. 20. *The change of support height in the loading test*

7 CONCLUSIONS

In this paper, a theoretical, analytical model of hydraulic support attitude based on the length of the front and rear columns is proposed, and a rigid body simulation model of hydraulic support is established

to verify the theoretical, analytical model. Three factors that may affect the attitude monitoring and control accuracy of hydraulic support, such as material elastic deformation, Axis pin connection clearance, and hydraulic cylinder force compression, are analysed. The influence of various factors on the attitude of hydraulic support is studied, and the following conclusions were obtained:

1. The theoretical analytical model of hydraulic support attitude is proposed, which can solve the attitude of hydraulic support through the length of the front and rear columns. Based on this algorithm, a method of attitude monitoring and control of hydraulic support based on column length is proposed.
2. The rigid body simulation model of hydraulic support is established to verify the theoretical analytical model. The maximum error of forward and inverse solutions is not more than 4.73114×10^{-5} %, which proves that the theoretical analytical results are accurate and reliable and also proves the correctness of the rigid body simulation model. The rigid body simulation model can be used as a hydraulic support attitude monitoring system without considering the elastic deformation of the material and the clearance of the pin connection unit.
3. The rigid-flexible coupling dynamic simulation model of hydraulic support is constructed. When the support height is 1700 mm, the elastic deformation of hydraulic support components leads to the error of support height of hydraulic support of -0.2412 mm. As the length of the front and rear columns gradually decreases, the hinge point force under the self-weight condition of the hydraulic support gradually increases, which leads to an increase in the support height error. The elastic deformation factor has a smaller impact on the support attitude when the support height of the hydraulic support is higher.
4. The rigid-flexible coupling dynamic simulation model of hydraulic support with clearance is constructed; the support height is 2490 mm, compared with the rigid body simulation results, the support height error is 2.2649 mm, and the axis pin connection clearance is a factor that must be considered in the attitude solution of the hydraulic support.
5. The rigid-flexible and mechanical-hydraulic coupling dynamics simulation model of the hydraulic support with clearance is established. In the loading test with a support height of 2500 mm, the hydraulic support's height is reduced by

90.8686 mm. When the hydraulic support attitude is adjusted, the theoretical flow calculation cannot be used, and the column length should be directly measured.

6. Through the comparative analysis of the support height error of hydraulic support under three different influencing factors of material elastic deformation, axis pin connection clearance, and hydraulic cylinder force compression, it can be concluded that among the three influencing factors, the hydraulic cylinder force compression has the greatest influence on the attitude of hydraulic support, and the material elastic deformation has the least influence. Compared with the other two factors, the influence of material elastic deformation is only 1/9 or less.

The research provides theoretical support for the monitoring and control of hydraulic support attitude, which is of great significance to promoting intelligent mining in coal mines.

The limitation of this paper lies in only studying the position and attitude of hydraulic support and cannot obtain the position and attitude information of the whole hydraulic support in space, such as yaw angle, roll angle and pitch angle, and only studies a single hydraulic support. There are two directions for future research. Direction 1: Study the attitude of a base or hydraulic support in space and obtain the attitude information of the whole support in space through a single component. Direction 2: Calculate the overall position and attitude of the hydraulic support group and monitor the overall position and attitude of the support group through the geometric relationship of the adjacent frame.

The changing working attitude of hydraulic support significantly affects the support's bearing characteristics and may even damage its structural components. To ensure efficient, safe, continuous, and stable production in a comprehensive mechanized coal mining face, intelligent monitoring and proper control of the wave pressure support attitude are crucial to prevent shearer top beam cutting, balance jack breakage, and excessive top beam inclination. Many scholars have studied the attitude of hydraulic support deeply, such as the design of mine hydraulic support height measurement system based on an inclination sensor published by Huang et al. [45], the design of hydraulic support posture dynamic monitoring and control system published by Lu et al. [46], the sensing and data processing technology of hydraulic support state published by Pang et al. [47], and the support posture and driving jack in the initial supporting stage published by Hu et al. [48]. These

studies try to use different inclination sensors and different filtering algorithms to analyse the support attitude perception results of hydraulic support, develop hydraulic support attitude and support height monitoring system, improve the perception accuracy of inclination sensors and the analysis efficiency of hydraulic support attitude. These researches are based on a large number of sensors for information fusion, which is costly and difficult to apply and popularize. The attitude analysis method of hydraulic support proposed in this paper only needs two groups of sensors to measure the length of the front and rear columns, and the attitude information of hydraulic support can be obtained, which is less in the number of sensors and low in cost and easy to popularize.

8 DISCUSSION

Much research has been conducted on the position and attitude monitoring of hydraulic support, but there are differences in the types, numbers, and installations of sensors, as well as research priorities and directions.

For example, Chen et al. [11] studied the fusion technology of wide-angle ultrasonic sensor and inclination sensor in Research on attitude monitoring method of advanced hydraulic support based on multi-sensor fusion, which was applied to attitude monitoring of advanced hydraulic support in harsh underground environments. They established a measurement model based on advanced hydraulic support kinematics and then proposed yaw angle and roll angle calculation algorithms based on ultrasonic ranging data to achieve multi-sensor-based advanced hydraulic support attitude monitoring. Chen's research [11] calculates the position of hydraulic support through a variety of sensors, and the number of sensors is large, the variety is large, and the cost is high, which is not conducive to practical application. This paper only needs two groups of sensors to measure the length of the front and rear columns. The number of sensors is small, the cost is low, and it is easy to be popularized. Lu et al. [18] proposed a method for attitude monitoring of hydraulic support in A portable support attitude sensing system for accurate attitude estimation of hydraulic support based on an unscented Kalman filter. According to the complementary characteristics of a magnetometer, accelerometer, and gyroscope, a supporting attitude sensing system composed of an inertial measurement unit and MEMS was designed. The attitude of hydraulic support is improved by the multi-sensor information fusion method, but the emphasis is on the yaw angle, roll angle, and pitch angle of hydraulic support in space. Both this paper

and Lu's research are aimed at the attitude of hydraulic support, but the object of this paper is the posture of hydraulic support itself, which has not been studied by Lu et al. [18].

9 ACKNOWLEDGEMENT

10 REFERENCE

[1] Wang, G., Liu, F., Pang, Y., Ren, H., Ma, Y. (2019). Intelligent coal mine-core technical support for high-quality development of coal industry. *Journal of China Coal Society*, vol. 44, no. 2, p. 349-357, **DOI:10.13225/j.cnki.jccs.2018.2041**. (in Chinese)

[2] Wang, G., Ren, H., Pang, Y., Cao, X., Zhao, G., Chen, H., Du, Y., Mao, S., Xu, Y., Ren, S., Cheng, J., Liu, S., Fan, J., Wu, Q., Meng, X., Yang, J., Yu, B., Xuan, H., Sun, X., Zhang, D., Wang, H. (2020). Advances in research and engineering of coal mine intelligent (primary stage) technology system. *Coal Science and Technology*, vol. 48, no. 7, p. 1-27, **DOI:10.13199/j.cnki.cst.2020.07.001**. (in Chinese)

[3] Liu, F., Cao, W., Zhang, J., Cao, G., Guo, L. (2021). Progress of scientific and technological innovation in China 's coal industry and the development direction of the 14th Five-Year Plan. *Journal of China Coal Society*, vol. 46, no. 1, p. 1-15, **DOI:10.13225/j.cnki.jccs.2021.0042**. (in Chinese)

[4] Bao, J., Zhang, Q., Ge, S., Hu, E., Yuan, X., Yang, Y., Yin, Y., Lu, Y. (2023). Key basic research and application practice of unmanned auxiliary transportation system in coal mine. *Journal of China Coal Society*, vol. 48, no. 2, p. 1085-1098, **DOI:10.13225/j.cnki.jccs.2022.1600**. (in Chinese)

[5] Zhang, K., Sun, Z., Liu, Y., Li, Y., Du, M., Ma, Y., Wei, X., Xu, Y., Wang, X., Yu, T., Ding, C. (2023). Research and experimental verification of advanced hydraulic support attitude perception method based on information fusion technology. *Journal of China Coal Society*, p. 1-14, **DOI:10.13225/j.cnki.jccs.2022.0621**. (in Chinese)

[6] Lian, Z., Yuan, X., Gao, F., Liao, Y., Guo, Y., Zhao, R. (2020). Network intelligent sensing control method of hydraulic support. *Journal of China Coal Society*, vol. 45, no. 6, p. 2078-2089, **DOI:10.13225/j.cnki.jccs.ZN20.0361**. (in Chinese)

[7] Ren, H., Zhao, G., Zhou, J., Wen, Z., Ding, Y., Li, S. (2020). Full pose measurement and virtual simulation control technology of intelligent mining equipment. *Journal of China Coal Society*, vol. 45, no. 3, p. 956-971, **DOI:10.13225/j.cnki.jccs.SJ20.0335**. (in Chinese)

[8] Li, S., Ren, H. (2020). Research status and prospect of pose measurement technology of ' three machines ' equipment in fully mechanized mining face. *Coal Science and Technology*, vol. 48, no. 9, p.218-226, **DOI:10.13199/j.cnki.cst.2020.09.028**. (in Chinese)

[9] Pang, Y., Liu, X., Wang, H., Jiang, Z., Guan, S., Zhang, Z., Wang, W. (2023). Analytical method of support attitude and height of hydraulic support based on jack stroke drive. *Journal of Mining & Safety Engineering*, p. 1-14. (in Chinese)

[10] Wang, X., Cui, T., Xie, J., Shen, H., Liu, Y., Wang, B. (2021). Virtual simulation method of hydraulic support motion considering pin clearance. *Coal science and technology*, vol. 49, no. 2, p. 186-193, **DOI:10.13199/j.cnki.cst.2021.02.022**. (in Chinese)

[11] Chen, H., Chen, H., Xu, Y., Zhang, D., Ma, Y., Mao, J. (2022). Research on attitude monitoring method of advanced hydraulic support based on multi-sensor fusion. *Measurement*, vol. 187, 110341, **DOI:10.1016/j.measurement.2021.110341**.

[12] Zhang, Y., Zhang, H., Gao, K., Xu, W., Zeng, Q. (2019). New method and experiment for detecting relative position and attitude of the hydraulic support. *IEEE Access*, vol. 7, p. 181842-181854, **DOI:10.1109/ACCESS.2019.2958981**.

[13] Liang, M., Fang, X., Li, S., Wu, G., Ma, M., Zhang, Y. (2019). A fiber Bragg grating tilt sensor for attitude monitoring of hydraulic supports in coal mine working face. *Measurement*, vol. 138, p. 305-313, **DOI:10.1016/j.measurement.2019.02.060**.

[14] Zeng, X., Meng, G., Zhou, J. (2018). Analysis on the pose and dynamic response of hydraulic support under dual impact loads. *International Journal of Simulation Modelling*, vol. 17, no. 1, p. 69-80, **DOI:10.2507/ijsimm17(1)412**.

[15] Ge, X., Xie, J., Wang, X., Liu, Y., Shi, H. (2020). A virtual adjustment method and experimental study of the support attitude of hydraulic support groups in propulsion state. *Measurement*, vol. 158, 107743, **DOI:10.1016/j.measurement.2020.107743**.

[16] Wang, B., Xie, J., Wang, X., Liu, S., Liu, Y. (2021). A new method for measuring the attitude and straightness of hydraulic support groups based on point clouds. *Arabian Journal for Science and Engineering*, vol. 46, p. 11739-11757, **DOI:10.1007/s13369-021-05689-2**.

[17] Yang, X., Wang, R., Wang, H., Yang, Y. (2020). A novel method for measuring pose of hydraulic supports relative to inspection robot using LiDAR. *Measurement*, vol. 154, p. 107452, **DOI:10.1016/j.measurement.2019.107452**.

[18] Lu, X., Wang, Z., Tan, C., Yan, H., Si, L., Wei, D. (2020). A portable support attitude sensing system for accurate attitude estimation of hydraulic support based on unscented Kalman filter. *Sensors*, vol. 20, no. 19, 5459, **DOI:10.3390/s20195459**.

[19] Wang, X., Liu, S., Wang, X., Xie, J., Wang, B., Wang, Z. (2022). Research and experiment on key technologies of intelligent monitoring of fully mechanized mining face driven by AR / VR fusion. *Journal of China Coal Society*, vol. 47, no. 2, p. 969-985, **DOI:10.13225/j.cnki.jccs.2021.1113**. (in Chinese)

[20] Wang, X., Xie, J., Hao, S., Li, J., Yang, Z., Ren, F., Bao, Q. (2020). Real-time virtual monitoring method and key technology of intelligent fully mechanized mining face. *Journal of China Coal Society*, vol. 45, no. 6, p. 1984-1996, **DOI:10.13225/j.cnki.jccs.zn20.0342**. (in Chinese)

[21] Szurgacz, D., Brodny, J. (2019). Tests of geometry of the powered roof support section. *Energies*, vol. 12, no. 20, 3945, **DOI:10.3390/en12203945**.

[22] Szurgacz, D., Brodny, J. (2020). Adapting the powered roof support to diverse mining and geological conditions. *Energies*, vol. 13, no. 2, 405, **DOI:10.3390/en13020405**.

[23] Chen, G., Zhang, Z., Kong, L., Wang, H. (2020). Analysis and validation of a flexible planar two degrees-of-freedom parallel manipulator with structural passive compliance. *Journal of Mechanisms and Robotics*, vol. 12, no. 1, 011011, **DOI:10.1115/1.4045036**.

[24] Hamida, I. B., Laribi, M. A., Mlika, A., Romdhane, L., Zeghloul, S., Carbone, G. (2021). Multi-objective optimal design of a cable driven parallel robot for rehabilitation tasks. *Mechanism and Machine Theory*, vol. 156, 104141, **DOI:10.1016/j.mechmachtheory.2020.104141**.

[25] Yiyang, L., Xi, J., Hongfei, B., Zhining, W., Liangliang, S. (2021). A general robot inverse kinematics solution method based on improved PSO algorithm. *IEEE Access*, vol. 9, p. 32341-32350, **DOI:10.1109/ACCESS.2021.3059714**.

[26] Bai, Y., Luo, M., Pang, F. (2021). An algorithm for solving robot inverse kinematics based on FOA optimized BP neural network. *Applied Sciences*, vol. 11, no. 15, 7129, **DOI:10.3390/app11157129**.

[27] Luo, G., Zou, L., Wang, Z., Lv, C., Ou, J., Huang, Y. (2021). A novel kinematic parameters calibration method for industrial robot based on Levenberg-Marquardt and Differential Evolution hybrid algorithm. *Robotics and Computer-Integrated Manufacturing*, vol. 71, 102165, **DOI:10.1016/j.rcim.2021.102165**.

[28] Feng, Z., Xie, J., Yan, Z., Mei, Z., Zheng, Z., Li, T. (2023). An information processing method of software and hardware coupling for VR monitoring of hydraulic support groups. *Multimedia Tools and Applications*, vol. 82, p. 19067-19089, **DOI:10.1007/s11042-022-14128-9**.

[29] Gong, W., Liao, Z., Mi, X., Wang, L., Guo, Y. (2021). Nonlinear equations solving with intelligent optimization algorithms: A survey. *Complex System Modeling and Simulation*, vol. 1, no. 1, p. 15-32, **DOI:10.23919/CSMS.2021.0002**.

[30] Nadeem, M., He, J.-H. (2021). He-Laplace variational iteration method for solving the nonlinear equations arising in chemical kinetics and population dynamics. *Journal of Mathematical Chemistry*, vol. 59, p. 1234-1245, **DOI:10.1007/s10910-021-01236-4**.

[31] Rasheed, M., Shihab, S., Rashid, T., Enneffati, M. (2021). Some step iterative method for finding roots of a nonlinear equation. *Journal of Al-Qadisiyah for Computer Science and Mathematics*, vol. 13, no. 1, p. 95-102, **DOI:10.29304/jqcm.2021.13.1.753**.

[32] David Müzel, S., Bonhin, E. P., Guimarães, N. M., Guidi, E. S. (2020). Application of the finite element method in the analysis of composite materials: A review. *Polymers*, vol. 12, no. 4, p. 818, **DOI:10.3390/polym12040818**.

[33] Guo, Q., Yao, W., Li, W., Gupta, N. (2021). Constitutive models for the structural analysis of composite materials for the finite element analysis: A review of recent practices. *Composite Structures*, vol. 260, 113267, **DOI:10.1016/j.compstruct.2020.113267**.

[34] Bagha, A. K., Bahl, S. (2021). Finite element analysis of VGCF/pp reinforced square representative volume element to predict its mechanical properties for different loadings. *Materials Today: Proceedings*, vol. 39, p. 54-59, **DOI:10.1016/j.matpr.2020.06.108**.

[35] Zeng, Q., Li, Y., Yang, Y. (2021). Dynamic analysis of hydraulic support with single clearance. *Strojniški vestnik - Journal of Mechanical Engineering*, vol. 67, no. 1-2, p. 53-66, **DOI:10.5545/sv-jme.2020.6998**.

[36] Kardani, N., Zhou, A., Nazem, M., Shen, S.-L. (2021). Improved prediction of slope stability using a hybrid stacking ensemble method based on finite element analysis and field data. *Journal of Rock Mechanics and Geotechnical Engineering*, vol. 13, no. 1, p. 188-201, **DOI:10.1016/j.jrmge.2020.05.011**.

[37] Duan, T., Wei, J., Zhang, A., Xu, Z., Lim, T.C. (2021). Transmission error investigation of gearbox using rigid-flexible coupling dynamic model: Theoretical analysis and experiments. *Mechanism and Machine Theory*, vol. 157, 104213, **DOI:10.1016/j.mechmachtheory.2020.104213**.

[38] Xie, Y., Zeng, Q., Jiang, K., Meng, Z., Li, Q., Zhang, J. (2022). Investigation of dynamic behaviour of four-leg hydraulic support under double-impact load. *Strojniški vestnik - Journal of Mechanical Engineering*, vol. 68, no. 6, p. 385-394, **DOI:10.5545/sv-jme.2022.54**.

[39] Ren, H., Zhang, D., Gong, S., Zhou, K., Xi, C., He, M., Li, T. (2021). Dynamic impact experiment and response characteristics analysis for 1: 2 reduced-scale model of hydraulic support. *International Journal of Mining Science and Technology*, vol. 31, no. 3, p. 347-356, **DOI:10.1016/j.ijmst.2021.03.004**.

[40] Meng, Z.S., Zhang, J.M., Xie, Y.Y., Lu, Z.G., Zeng, Q.L. (2021). Analysis of the force response of a double-canopy hydraulic support under impact loads. *International Journal of Simulation Modelling*, vol. 20, p. 766-777, **DOI:10.2507/IJSIMM20-4-CO18**.

[41] Guo, C., Mao, J., Xie, M. (2022). Analysis of energy absorption characteristics of corrugated top beams of anti-impact hydraulic supports. *Alexandria Engineering Journal*, vol. 61, no. 5, p. 3757-3772, **DOI:10.1016/j.aej.2021.08.077**.

[42] Liu, Z., Li, P., Jiang, J., Liu, B. (2021). Research on vibration characteristics of mill rolls based on nonlinear stiffness of the hydraulic cylinder. *Journal of Manufacturing Processes*, vol. 64, p. 1322-1328, **DOI:10.1016/j.jmapro.2021.02.063**.

[43] Jaiswal, S., Sopanen, J., Mikkola, A. (2021). Efficiency comparison of various friction models of a hydraulic cylinder in the framework of multibody system dynamics. *Nonlinear Dynamics*, vol. 104, p. 3497-3515, **DOI:10.1007/s11071-021-06526-9**.

[44] Stawinski, L., Skowronska, J., Kosucki, A. (2021). Energy efficiency and limitations of the methods of controlling the hydraulic cylinder piston rod under various load conditions. *Energies*, vol. 14, no. 23, p. 7973, **DOI:10.3390/en14237973**.

[45] Huang, H., Wang, F., Tian C., Zhao, W., Cao, G. (2018). Design of mine hydraulic support height measurement system based on inclination sensor. *Coal Science and Technology*, vol. 46, no. 03, p. 124-129+193, **DOI:10.13199/j.cnki.cst.2018.03.021**. (in Chinese)

[46] Lu, T., Ma, P., Feng, Z., Yu, J. (2014). Design of Dynamic Monitoring and Control System for Hydraulic Support Attitude. *Coal Science and Technology*, vol. 42, no. S1, p. 169 -170,172, **DOI:10.13199/j.cnki.cst.2014.s1.071**. (in Chinese)

[47] Pang, Y. (2021). Perception and data processing technology of hydraulic support support. *Industry and Mine Automation*, vol. 47, no. 11, p. 66-73, **DOI:10.13272/j.issn.1671-251x.2021040061**. (in Chinese)

[48] Hu, X., Liu, X. (2021). The mapping and adjustment strategy of support pose and driving jack in initial bracing stage. *Journal of Mining and Safety Engineering*, vol. 38, no. 04, p. 666 -677, **DOI:10.13545/j.cnki.jmse.2020.0158**. (in Chinese)